Contribution from the Chemistry Department,
University of Houston, University Park, Houston, Texas 77004

Activation of Triiron Clusters by Electron Transfer. Radical Anions and Dianions of $Fe_3(\mu_3\text{-}PPh)_2(CO)_9$ and Its Derivatives

H. H. Ohst and J. K. Kochi*

Received November 11, 1985

The bicapped triiron cluster $Fe_3(\mu_3\text{-}PPh)_2(CO)_9$ (A) undergoes successive, 1-electron reductions to produce the anion radical $A^{-\cdot}$ and the diamagnetic dianion A^{2-} at the reversible potentials $E^0 = -0.79$ and -1.30 V, respectively. The anion radical suffers rapid ligand substitution by CO replacement with various phosphorus-centered ligands. Transient ESR spectroscopy establishes the interconversion between two isomeric forms of the anion radicals that are described as unopened ($C^{-\cdot}$) and opened ($C_i^{-\cdot}$) structures. The opening and reclosing of the cluster framework of the anion radical by slippage of the μ_3-PPh cap plays an important role in the mechanism of ligand substitution. The latter is incorporated into the general scheme for electron-transfer catalysis of ligand substitution induced by the partial reduction of $Fe_3(PPh)_2(CO)_9$ in the presence of nucleophiles. The phosphinidene cap also plays an important role in the reaction of the dianion. Thus, protonation of A^{2-} with acetic acid at -78 °C occurs readily at the phosphinidene bridge, leading to the formation of a μ_2-phosphide center by scission of the Fe–P bond. The same product is derived by hydridic attack on the neutral cluster. The parallel behavior of all three species, A, $A^{-\cdot}$, and A^{2-}, thus underscores the critical role of the bridging phosphinidene cap in cluster reactivity.

Introduction

Transition-metal clusters offer access to various oxidation and reduction levels as a result of contiguous metal centers.[1-3] The chemical reactivity of such oxidized and reduced species should provide an expanded view of cluster behavior. Among the various systems, the triiron cluster $Fe_3(PPh)_2(CO)_9$ has been known for some time,[4] and various routes for its preparation have been described.[4-11] The extraordinary robustness of this bicapped triiron cluster is shown by its survival following the extensive thermal degradation of various phosphorus-bridged iron carbonyl clusters.[5] The thermal reactions of $Fe_3(PPh)_2(CO)_9$, such as ligand substitution, require elevated temperatures. For example, the replacement of CO by trimethyl phosphite occurs only in refluxing xylene and then produces a random mixture of mono-, bis-, and tris-substitution products in low yields.[4] Similarly, the substitution of a CO ligand by acetonitrile was observed after 8 h in the refluxing solvent.[7] The thermal incorporation of additional iron carbonyl fragments into the triiron framework to afford the tetranuclear clusters $Fe_4(PPh)_2(CO)_{11}$ and $Fe_4(PPh)_2(CO)_{12}$ has been examined in detail.[5c,d] The triiron cluster is inert to water and anhydrous hydrogen chloride.[6,13] However, inconsistent results have been obtained with nucleophiles. Thus, it has been reported to be unreactive toward butyllithium,[6] but sodium borohydride converts a μ_3-phosphinidene bridge to a μ_2-phosphide unit.[14] Moreover, the nucleophilic attack on a coordinated CO by phenyllithium is reported to yield a benzoyl derivative.[15] Following from our studies of the electron-transfer catalysis of cluster substitution,[16] we now examine the behavior of $Fe_3(PPh)_2(CO)_9$ toward various phosphorus-centered nucleophiles and the nature of the anion radicals and dianions formed as reactive intermediates.

Results and Discussion

Reduction of the triiron cluster $Fe_3(PPh)_2(CO)_9$ (A) by electron transfer is best considered from its cyclic voltammetric behavior shown in Figure 1, in which the reversible, 1-electron CV waves at $E_{1/2} = -0.79$ and -1.30 V vs. SCE correspond to the formation of the anion radical $A^{-\cdot}$ and dianion A^{2-}, respectively.

$$\underset{A}{Fe_3(PPh)_2(CO)_9} \overset{-0.79\ V}{\rightleftharpoons} \underset{A^{-\cdot}}{Fe_3(PPh)_2(CO)_9^{-\cdot}} \overset{-1.30\ V}{\rightleftharpoons} \underset{A^{2-}}{Fe_3(PPh)_2(CO)_9^{2-}} \quad (1)$$

I. Preparation and Isomeric Structures of the Anion Radicals from $Fe_3(PPh)_2(CO)_9$. The bulk electrochemical reduction of orange-red triiron cluster A at -0.80 V in tetrahydrofuran (THF) containing 0.3 M tetra-*n*-butylammonium perchlorate (TBAP) consumes 1 faraday of charge and yields a dark green solution of $A^{-\cdot}$. The infrared spectrum of $A^{-\cdot}$ shows a pair of prominent absorption bands at 1990 and 1977 cm^{-1}, which are similar to those at 2043 and 2020 cm^{-1} in the parent cluster A (Table I). The shift of $\sim$50 cm^{-1} to lower energy upon reduction of the intact cluster is similar to that observed in a tricobalt system.[17] $A^{-\cdot}$ can also be prepared in the absence of extra salt by chemical reduction with cobaltocene, i.e.

$$Fe_3(PPh)_2(CO)_9 + Cp_2Co \rightarrow Cp_2Co[Fe_3(PPh)_2(CO)_9] \quad (2)$$

which has a reduction potential $E^0(Cp_2Co) = -0.95$ V.[18] Since all attempts to isolate $A^{-\cdot}$ as a pure salt were unsuccessful, the further studies were carried out with the anion radical prepared in situ by chemical reduction.

The ESR spectrum of anion radical $A^{-\cdot}$ taken immediately upon reduction by cobaltocene in acetonitrile consists of a binomial 1:2:1 triplet due to the hyperfine splitting from two equivalent phos-

(1) Vahrenkamp, H. *Adv. Organomet. Chem.* **1983**, *22*, 169.
(2) Lemoine, P. *Coord. Chem. Rev.* **1982**, *47*, 55.
(3) Geiger, W. E.; Connelly, N. G. *Adv. Organomet. Chem.* **1985**, *24*, 2.
(4) Treichel, P. M.; Dean, W. K.; Douglas, W. M. *Inorg. Chem.* **1972**, *11*, 1609.
(5) (a) Lang, H.; Zsolnai, L.; Hüttner, G. *J. Organomet. Chem.* **1985**, *282*, 23. (b) Brauer, D. J.; Hietkamp, S.; Sommer, H.; Stelzer, O.; Müller, G.; Krüger, C. *J. Organomet. Chem.* **1985**, *288*, 35. (c) Vahrenkamp, H.; Wucherer, E. J.; Wolters, D. *Chem. Ber.* **1983**, *116*, 1219. (d) Müller, M.; Vahrenkamp, H. *Chem. Ber.* **1983**, *116*, 2311.
(6) Lampin, J. P.; Mathey, F. *C. R. Seances Acad. Sci., Ser. C* **1976**, *282*, 979.
(7) Kouba, J. K.; Muetterties, E. L.; Thompson, M. R.; Day, V. W. *Organometallics* **1983**, *2*, 1065.
(8) Cook, S. L.; Evans, J.; Gray, L. R.; Webster, M. *J. Organomet. Chem.* **1982**, *236*, 367.
(9) Patel, V. D.; Taylor, N. J.; Carty, A. J. *J. Chem. Soc., Chem. Commun.* **1984**, 99.
(10) Hietkamp, S.; Stelzer, O.; Engelhardt, M.; Hagela, G. *Z. Anorg. Allg. Chem.* **1981**, *475*, 131.
(11) Bartsch, R.; Hietkamp, S.; Morton, S.; Stelzer, O. *J. Organomet. Chem.* **1981**, *222*, 263.
(12) Hüttner, G.; Mohr, G.; Friedrich, P.; Schmid, H. G. *J. Organomet. Chem.* **1978**, *160*, 59.
(13) Kouba, J. K.; Pierce, J. L.; Walton, R. A. *J. Organomet. Chem.* **1980**, *202*, C105.
(14) O'Connor, J. P. Ph.D. Thesis, University of Wisconsin, Madison, WI, 1977.
(15) Williams, G. D.; Geoffroy, G. L.; Whittle, R. R. *J. Am. Chem. Soc.* **1985**, *107*, 729.
(16) Richmond, M. G.; Kochi, J. K. *Inorg. Chem.* **1986**, *25*, 656.
(17) Peake, B. M.; Robinson, B. H.; Simpson, J.; Watson, D. J. *Inorg. Chem.* **1977**, *16*, 405.
(18) Kölle, U. *J. Organomet. Chem.* **1978**, *152*, 225.

0020-1669/86/1325-2066$01.50/0

Table I. Infrared Spectra of Triiron Clusters

triiron cluster	solvent	ν(CO) str freq[a]
$Fe_3(\mu_3\text{-}PPh)_2(CO)_9$ (A)	THF	2073 (w), 2043 (s), 2020 (s), 2003 (m), 1990 (m), 1959 (w)
$Fe_3(\mu_3\text{-}PPh)_2(CO)_9^{-\cdot}$ ($A^{-\cdot}$)	THF	2029 (w), 1990 (s), 1977 (s), 1947 (m), 1929 (m)
$Fe_3(\mu_3\text{-}PPh)_2(CO)_9^{2-}$ (A^{2-})	THF	1998 (m), 1948 (s), 1919 (s), 1872 (m), 1817 (m), 1783 (w)
$Fe_3(\mu_3\text{-}PPh)(\mu_2\text{-}PPh)(CO)_9^{-\cdot}$ ($A_i^{-\cdot}$)	CH_3CN	2031 (w), 1998 (s), 1960 (s), 1932 (m), 1898 (w)
$Fe_3(\mu_3\text{-}PPh)(\mu_2\text{-}PHPh)(CO)_9^{-}$ (AH^{-})	THF	2031 (w), 1997 (s), 1962 (s), 1954 (s), 1931 (w), 1900 (w)
$Fe_3(\mu_3\text{-}PPh)(\mu_2\text{-}PHPh)(CO)_9^{-}$ (AH'^{-})	THF	2031 (w), 1997 (s), 1962 (s), 1954 (s), 1931 (w), 1900 (w)
$Fe_3(\mu_3\text{-}PPh)(\mu_2\text{-}PMePh)(CO)_9^{-}$ (AMe^{-})	THF	2028 (w), 1993 (s), 1960 (s), 1950 (s), 1927 (w), 1896 (w)

[a] In cm^{-1}. Intensities: (s) strong, (m) medium, (w) weak.

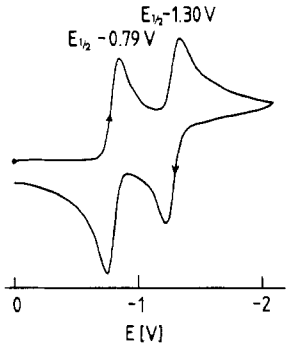

Figure 1. Initial cathodic scan cyclic voltammogram of $Fe_3(PPh)_2(CO)_9$ in THF containing 0.3 M TBAP at 500 mV s^{-1} and 25 °C.

phinidene bridges in $A^{-\cdot}$ (a_P = 13.3 G, $\langle g \rangle$ = 2.019). This ESR spectrum (Figure 3a, vide infra) coupled with the similar infrared spectra of A and $A^{-\cdot}$ (Table I) indicates that electron attachment has occurred on A with minimal alteration of the triiron cluster, i.e.

(3)

Accordingly, we consider the anion radical $A^{-\cdot}$ to have the same skeletal framework as its precursor. The reversible CV wave in Figure 1 and the bulk electrochemical oxidation of $A^{-\cdot}$ to regenerate parent triiron cluster A in high yields verify this structural assignment.

When anion radical $A^{-\cdot}$ is allowed to stand (in acetonitrile solution), the ESR spectrum in Figure 3a slowly evolves to that shown in Figure 2a (vide infra). The structural transformation of the anion radical accompanying this change corresponds to an isomerization, since oxidation of this solution regenerates parent cluster A. The new ESR spectrum in Figure 2a clearly consists of a doublet of doublets at $\langle g \rangle$ = 2.039 with hyperfine splittings of 25.3 and 3.4 G arising from two structurally different types of phosphorus centers. Such a transformation will result from the simple scission of a Fe–P bond in the cluster to render the pair of phosphinidene caps inequivalent, e.g.

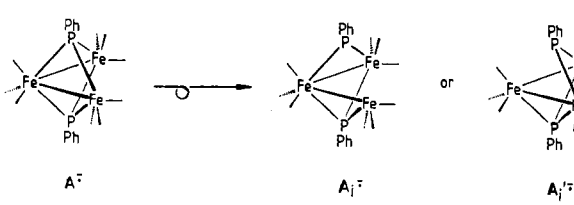

(4)

The structural forms $A_i^{-\cdot}$ and $A_i'^{-\cdot}$ are designated as *opened* triiron clusters since one of the phosphinidene bridges has undergone a $\mu_3 \rightarrow \mu_2$ ring opening. Further studies of phosphine derivatives, to be described in the following section, will favor opened structure $A_i^{-\cdot}$ shown on the left.

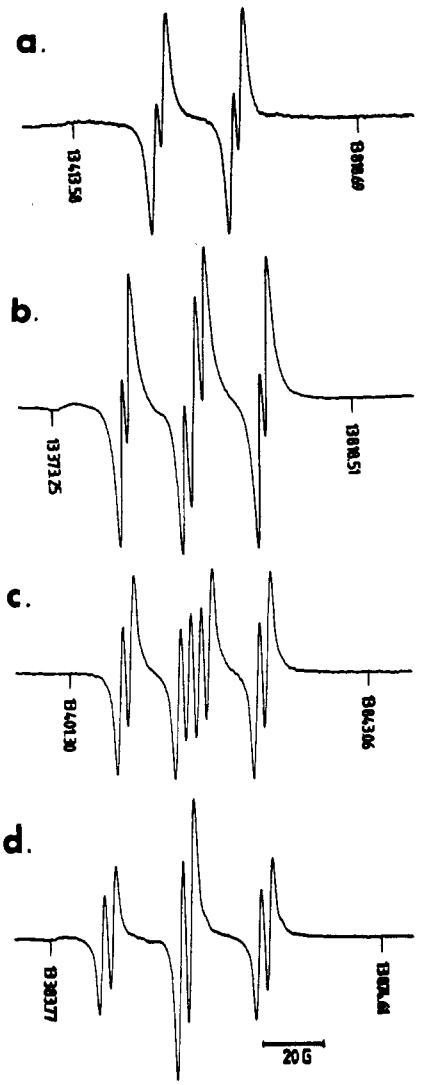

Figure 2. ESR spectra (X-band) of the *opened* anion radicals $Fe_3(\mu_3\text{-}PPh)(\mu_2\text{-}PPh)(CO)_8L^{-\cdot}$ in acetonitrile at 25 °C where (a) L = CO, (b) L = PEt_3, (c) L = PPh_3, and (d) L = $P(O\text{-}i\text{-}Pr)_3$. Proton NMR field markers are in kHz.

II. Ligand Substitution of the Anion Radical $Fe_3(PPh)_2(CO)_9^{-\cdot}$. Treatment of triiron anion radical $A_i^{-\cdot}$ with triethylphosphine in acetonitrile led to the instantaneous evolution of carbon monoxide and concomitant ligand substitution of the cluster, i.e.

$$\underset{A_i^{-\cdot}}{Fe_3(PPh)_2(CO)_9^{-\cdot}} + PEt_3 \xrightarrow{\text{fast}} \underset{B_i^{-\cdot}}{Fe_3(PPh)_2(CO)_8PEt_3^{-\cdot}} + CO \qquad (5)$$

The ligand substitution in eq 5 is rapid and occurs within the time span required for mixing, as shown by the spontaneous appearance of the ESR spectrum in Figure 2b. The identical ESR spectrum is obtained from the corresponding reduction of the mono(triethylphosphine) derivative B, $Fe_3(PPh)_2(CO)_8PEt_3$, of known structure.[19] The ESR spectrum in Figure 2b consists of a doublet

Table II. ESR Parameters of the Triiron Clusters $Fe_3(CO)_8(\mu_3\text{-PPh})(\mu_2\text{-PPh})L^{-\cdot}$[a]

	^{31}P hyperfine splitting, G			free ligand	
L	μ_3-P[b]	μ_2-P[b]	L[b,c]	cone angle,[d] deg	$\Delta\delta(^{13}C)$[e]
CO	25.3	3.4			
PPh_3	25.5	3.4	18.8 (18.5)	145	4.30
$P(p\text{-}ClC_6H_4)_3$	25.5	3.5	18.5	145	3.54
$P(p\text{-}MeC_6H_4)_3$	25.5	3.5	19.2	145	4.50
$P(p\text{-}MeOC_6H_4)_3$	25.3	3.5	19.5	145	4.43
$^1/_2(PPh_2CH_2)_2$	25.5	3.3	19.0 (20.4)		
PPh_2Et	25.3	3.5	19.2	140	4.78
PPh_2Me	25.3	3.3	19.6 (18.8)	136	4.53
$PPhEt_2$	25.3	3.4	19.7	136	5.36
$PPhMe_2$	24.8	3.2	20.5	122	4.76
PEt_3	24.8	3.4	20.3	132	5.54
$P(i\text{-}Pr)_3$	25.3	3.2	18.9	160	6.20
PBu_3	24.8	3.3	20.3	132	5.69
$P(c\text{-}C_6H_{11})_3$	25.3	3.2	18.5	170	6.32
$PPh_2(OBu)$	24.9	3.5	20.9		4.30
$PPh(OBu)_2$	24.8	3.5	23.2	116	4.20
$P(OPh)_3$	25.8	3.8	23.1 (25.0)	128	1.69
$P(OMe)_3$	25.3	3.5	25.3	107	3.18
$P(O\text{-}i\text{-}Pr)_3$	25.3	3.3	25.3	130	3.10
$AsPh_3$	26.0	3.3	17.0 (17.6)[f]		

[a] From $Fe_3(CO)_9(\mu_3\text{-PPh})_2^{-\cdot}$ and ligand L in acetonitrile at 25 °C. All $\langle g\rangle$ values = 2.040. ΔH_{pp} = 1.7 G. [b] Doublet splitting. [c] Values in parenthesis for L in $Fe(CO)_3L_2^{+\cdot}$ ($\langle g\rangle$ = 2.045–2.054) from: Baker, P. K.; Connelly, N. G.; Jones, B. M. R.; Maher, J. P.; Somers, K. R. *J. Chem. Soc., Dalton Trans.* **1980**, 579. [d] Tolman, C. A. *Chem. Rev.* **1977**, *77*, 313. [e] Bodner, G. M.; May, M. P.; McKinney, L. E. *Inorg. Chem.* **1980**, *19*, 1957. [f] 1:1:1:1 quartet for ^{75}As ($I = {}^3/_2$).

(a_P = 24.8 G) of doublets (a_P = 3.4 G) of doublets (a_P = 20.3 G). The hyperfine splittings of the first two doublets are essentially the same as those of precursor $A_i^{-\cdot}$ and are thus assigned to the μ_3- and μ_2-phosphinidene caps, respectively. Such a direct structural relationship of $A_i^{-\cdot}$ and $B_i^{-\cdot}$ is also evident from their same $\langle g\rangle$ values (Table II). The triethylphosphine ligand in $B_i^{-\cdot}$ shows the doublet splitting of a_P = 20.3 G.

The treatment of the anion radical ($A_i^{-\cdot}$) of $Fe_3(PPh)_2(CO)_9^{-\cdot}$ with various types of phosphorus-centered nucleophiles leads to a series of anion radicals $C_i^{-\cdot}$ that are closely related to $B_i^{-\cdot}$ in eq 5. The ESR spectra for the triphenylphosphine and triisopropyl phosphite analogues are also presented in Figure 2, parts c and d, respectively, to illustrate the various phosphorus splittings associated with such *opened* anion radicals. In each case, the hyperfine splitting pattern consists of three doublets (Table II), two of which remain relatively constant at $a_P \sim 25$ and ~ 3.5 G and are diagnostic of the μ_3- and μ_2-phosphinidene caps in the opened parent cluster. (Compare Figure 2a.) The third doublet, $a_P(L)$, varies systematically with structural changes of the phosphorus ligand. Indeed, the magnitudes of these phosphorus hyperfine splittings $a_P(L)$ in anion radicals $C_i^{-\cdot}$ are strikingly similar to those previously observed in the cation radicals of the 5-coordinate iron carbonyls $Fe(CO)_3L_2^{+\cdot}$.[20,21] For example, for the derivatives with L = PPh_3, PPh_2Et, and $P(OPh)_3$, the values of a_P = 18.5, 18.8, and 25.0 G, respectively, are comparable to those listed in Table II.[20] Furthermore, the 1:1:1:1 quartet splitting of 17.6 G arising from the isotopic ^{75}As ($I = {}^3/_2$) in the arsine derivative $Fe(CO)_3(AsPh_3)_2^+$ is quite similar to a_{As} = 17.0 G in

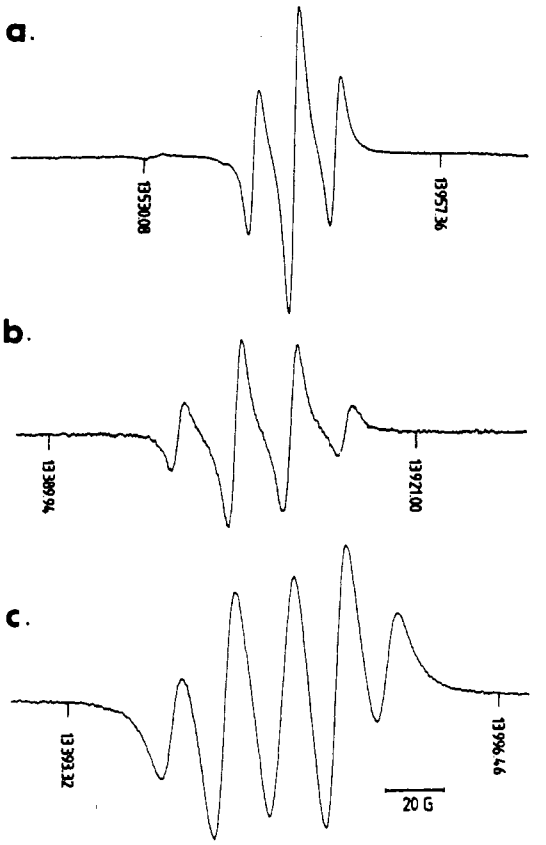

Figure 3. ESR spectra of the *unopened* anion radicals $Fe_3(\mu_3\text{-PPh})_2(CO)_8L^{-\cdot}$ in THF at 25 °C when (a) L = CO, (b) L = PEt_3, and (c) L = $P(OMe)_3$. Proton NMR field markers are in kHz.

the $C_i^{-\cdot}$ isomer of $Fe_3(PPh)_2(CO)_8AsPh_3^{-\cdot}$ (see Table II). We also note that the 17-electron iron center in $Fe(CO)_3L_2^+$ is substitutionally more related to the basal Fe(1) position than the apical Fe(2) position in the triiron cluster, as shown by a comparison of structures $A_i^{-\cdot}$ and $A_i'^{-\cdot}$ presented in eq 4. Finally, the $\langle g\rangle$ value of 2.040 for triiron anion radicals $C_i^{-\cdot}$ (Table II) accords with $\langle g\rangle$ = 2.049 ± 0.004 found in $Fe(CO)_3L_2^+$.[20] Accordingly, we proceed in our discussion with structure $C_i^{-\cdot}$.

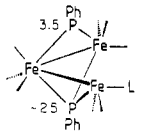

$C_i^{-\cdot}$

where L represents the various phosphorus-centered ligands identified in Table II. [We hope that isotopic (^{57}Fe) labeling of the triiron cluster will eventually help to establish this structural assignment.]

Opened anion radicals $C_i^{-\cdot}$ of the substituted triiron clusters are subject to both steric and electronic influences of the P substituents. For example, if one considers the series of trialkylphosphines R_3P with R = ethyl, *n*-butyl, isopropyl, and cyclohexyl, the value of $a_P(L)$ decreases with increasing cone angle of the ligand[22] (see Table II). Indeed, with the very bulky tri-*o*-tolyl phosphite, we were not able to observe a change in the ESR spectrum of $A_i^{-\cdot}$, which we interpret as an absence of substitution owing to the size of this ligand. Electronic effects derive from para-substituted triarylphosphine with constant cone angles. For this series, the value of $a_P(L)$ increases with the electron-donor ability of the phosphines, as measured by either $\delta(^{13}C)$ for $Ni(CO)_3L$[23] or Hammett σ values[24] in the order *p*-Cl < H < *p*-CH_3

(19) (a) For a preliminary report, see: Ohst, H. H.; Kochi, J. K. *J. Chem. Soc., Chem. Commun.* **1986**, 121. (b) See also: Ohst, H. H.; Kochi, J. K. *J. Am. Chem. Soc.*, in press. (c) For the step involving CO loss, see ref 19b.

(20) Baker, P. K.; Connelly, N. G.; James, B. M. R.; Maher, J. P.; Somers, K. R. *J. Chem. Soc., Dalton Trans.* **1980**, 579.

(21) See also: (a) Lappert, M. F.; MacQuitty, J. J.; Pye, P. L. *J. Chem. Soc., Dalton Trans.* **1981**, 1583. (b) Bagchi, R. N.; Bond, A. M.; Heggie, C. L.; Henderson, T. L.; Mocellin, E.; Seikel, R. A. *Inorg. Chem.* **1983**, *22*, 3007.

(22) Tolman, C. A. *Chem. Rev.* **1977**, *77*, 313.

(23) Bodner, G. M.; May, M. P.; McKinney, L. E. *Inorg. Chem.* **1980**, *19*, 1951.

Table III. ESR Parameters for the Triiron Clusters $Fe_3(CO)_8(\mu_3\text{-}PPh)_2L^{-\cdot}$[a]

L	^{31}P hyperfine splitting, G: μ_3-P[b]	P(L)[c]	⟨g⟩	ΔH_{pp}[d]
PEt_3	18.3	18.3	2.027	4.5
$P(OMe)_3$	17.8	36.0	2.023	6.5
$^1/_2(PPh_2CH_2)_2$	17.0	77.5	2.020	7.0
PPh_3	17.5	79.5	2.021	4.0
$^1/_2(PPh_2CH_2)_2$[e]	13.5	0	2.019	4.0
$(PPh_2CH_2)_2$[f]	12.0	81.0	2.020	3.5

[a] From the reduction of $Fe_3(CO)_8(\mu_3\text{-}PPh)_2L$ with 1% sodium amalgam in THF at 25 °C. [b] 1:21:1 triplet. [c] Doublet. [d] Peak to peak line width in G. [e] Mono-substitution on Fe(2) from the ESR spectrum in Figure 4c. [f] Bis-substitution from reduction of E, as shown by the ESR spectrum in Figure 4d.

< p-CH_3O. Such trends accord with the spin density on an unsaturated 17-electron iron center such as that on anion radical $A_i^{-\cdot}$ (vide supra) and on $Fe(CO)_3L_2^{+\cdot}$ examined earlier. Both effects, less steric bulk and greater donor ability, are parallel in the series PPh_3, PPh_2Et, $PPhEt_2$, and PEt_3 and are reflected in the monotonic change in $a_P(L)$.[28] The largest values of $a_P(L)$ are shown by phosphites, which have relatively small cone angles but are also weak donors. An enhanced mesomeric effect arising from the lone pairs on oxygen may be responsible for the increased spin density of the ligand in this series of anion radicals.

For comparison, the *unopened* anion radicals of the triethylphosphine and trimethyl phosphite derivatives were prepared directly by sodium amalgam reduction in tetrahydrofuran. The ESR spectrum of the trimethyl phosphite derivative in THF solution (Figure 3c) consists of a triplet (a_P = 17.8 G) of doublets (a_P = 36.0 G) at ⟨g⟩ = 2.023 (Table III). The ⟨g⟩ value and the triplet splitting are akin to those observed in the unopened parent, $A^{-\cdot}$, the ESR spectrum of which is included in Figure 3a. The ESR parameters for $A^{-\cdot}$ together with those obtained from the reduction of the trimethyl phosphite, 1,2-(diphenylphosphino)ethane (diphos, mono-dentate), and triphenylphosphine derivatives C are included in Table III. In each case, the hyperfine splitting pattern consists of a binomial 1:2:1 triplet of doublets. The triplet splitting is rather constant, $a_P = 15 \pm 3$ G in this series of anion radicals (Table III). Indeed, the ⟨g⟩ value and the triplet splittings are similar to those observed for the parent $A^{-\cdot}$ in eq 3. Accordingly, the triplet splitting is assigned to the pair of equivalent μ_3-phosphinidene caps in an analogous *unopened* structure, i.e.

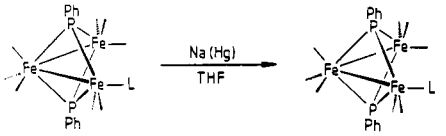

C C$^{-\cdot}$ (6)

where L represents a phosphorus-centered ligand. The involvement of extensive electron delocalization in the unopened cluster is indicated by the ⟨g⟩ values of 2.02 (Table II), which are close to ⟨g⟩ = 2.0016 observed for $Fe_3(CO)_{12}^{-\cdot}$.[25,26] It is noteworthy that the magnitude of the ligand splitting $a_P(L)$ in $C^{-\cdot}$ increases dramatically in the series $PEt_3 \ll P(OMe)_3 \ll PPh_3$, which is in marked contrast with the slight variation of $a_P(L)$ in isomeric $C_i^{-\cdot}$ (see Table II).

III. Anion Radicals in Ligand Substitution of the Triiron Cluster $Fe_3(PPh)_2(CO)_9$ by Electron-Transfer Catalysis. The anion radicals described above are the principal intermediates in the electron-transfer catalysis (ETC) of ligand substitution. For example, when $Fe_3(PPh)_2(CO)_9$ (A) was partially reduced to $Fe(PPh)_2(CO)_9^{-\cdot}$ by passage of a small cathodic current at −0.80 V in the presence of triphenylphosphine, the monosubstitution product C was isolated in 45% yield within 2 h at room temperature, i.e.[19]

$$\underset{A}{Fe_3(PPh)_2(CO)_9} + PPh_3 \xrightarrow{-0.80\ V} \underset{C}{Fe_3(PPh)_2(CO)_8PPh_3} + CO \quad (7)$$

(Note that the corresponding ligand substitution by the conventional thermal process does not occur at this temperature.[4]) The analogous mono-substitution product, D, from the diphosphine $Ph_2PCH_2CH_2PPh_2$ (diphos) was obtained under similar conditions. The bis-substitution product, E, of diphos was obtained when the charge was first passed at −0.80 V and then at −1.10 V, as described in Table IV. The potentials determine the selectivity in ligand substitution by selecting the particular triiron cluster to be reduced to its anion radical.[19,27] The potentials for the various triiron clusters were determined by cyclic voltammetry and are listed in Table V.

Mechanistic studies of electron-transfer catalysis for ligand substitution in general of a metal carbonyl M(CO) established the propagation sequence shown in Scheme I.[27,28] As applied

Scheme I

$$M(CO)^{-\cdot} + L \xrightarrow{(a)} M(L)^{-\cdot} + CO \quad (8)$$

$$M(L)^{-\cdot} + M(CO) \xrightarrow{(b)} M(L) + M(CO)^{-\cdot} \quad (9)$$

to the triiron clusters pertinent to this study, Scheme I emphasizes the importance of (a) ligand substitution in the anion radical $Fe_3(PPh)_2(CO)_9^{-\cdot}$ in eq 8 and (b) its electron transfer in eq 9. The driving force, ΔG, for the latter is readily ascertained from the relative reduction potentials of reactant A and product C in Table V. Crucial to the success of ETC is the substitutional lability of anion radical $A^{-\cdot}$ by the pathway summarized in Scheme II.[19]

Table IV. ETC Ligand Substitution of $Fe_3(PPh)_2(CO)_9$[a]

added ligand	E_p,[b] V	charge passed[c]	product (yield, %)
PPh_3	−0.80	0.2	$Fe_3(PPh)_2(CO)_8PPh_3$ (45)
$(Ph_2PCH_2)_2$	−0.80	0.1	$Fe_3(PPh)_2(CO)_8$(diphos) (38)
$(Ph_2PCH_2)_2$	−0.80	0.1	$Fe_3(PPh)_2(CO)_7$(diphos) (18)
	−1.10	0.6	

[a] In 25 mL of THF containing 0.3 mmol of $Fe_3(PPh)_2(CO)_9$ (A), 0.6 mmol of ligand, and 0.3 M tetra-*n*-butylammonium perchlorate at 25 °C. [b] Electrode potential for cluster reduction. [c] Faradays of charge passed relative to A charged.

Table V. Cyclic Voltammetry of Triiron Clusters[a]

triiron cluster	redn[b]: $E_{1/2}(1)$	redn[b]: $E_{1/2}(2)$	oxidn: E_p[c]
$Fe_3(PPh)_2(CO)_9$ (A)	−0.79	−1.30	1.37
$Fe_3(PPh)_2(CO)_8PPh_3$ (C)	−1.01	−1.62	1.09
$Fe_3(PPh)_2(CO)_8(Ph_2PCH_2)_2$ (D)	−1.06	−1.60	1.18
$Fe_3(PPh)_2(CO)_7(Ph_2PCH_2)_2$ (E)	−1.32	−2.01[d]	0.86

[a] In THF containing 1×10^{-3} M triiron cluster and 0.3 M TBAP at 100 mV s^{-1}. [b] Potentials are in V vs. SCE. $E_{1/2}$ from a pair of reversible 1-electron CV waves. [c] Irreversible anodic peak potential in V vs. SCE. [d] Irreversible cathodic peak potential.

(24) Lowry, T. H.; Richardson, K. S. *Mechanism and Theory in Organic Chemistry*, 2nd ed.; Harper and Row: New York, 1981; p 130 ff.
(25) (a) Dawson, P. A.; Peake, B. M.; Robinson, B. H.; Simpson, J. *Inorg. Chem.* **1980**, *19*, 465. (b) Miholova, D.; Klima, J.; Vlcek, A. *Inorg. Chim. Acta* **1978**, *27*, L67.
(26) See also: (a) Krusic, P. J.; San Filippo, J., Jr.; Hutchinson, B.; Hance, R. L.; Daniels, L. M. *J. Am. Chem. Soc.* **1981**, *103*, 2129. (b) Peake, B. M.; Robinson, B. H.; Simpson, J.; Watson, D. J. *J. Chem. Soc., Chem. Commun.* **1974**, 945.
(27) (a) Darchen, A.; Mahe, C.; Patin, H. *Nouv. J. Chim.* **1982**, *6*, 539. (b) Darchen, A.; Mahe, C.; Patin, H. *J. Chem. Soc., Chem. Commun.* **1982**, 243. (c) Richmond, M. G.; Kochi, J. K. In ref 16. (d) Bezems, G. J.; Rieger, P. H.; Visco, S. *J. Chem. Soc., Chem. Commun.* **1981**, 265. (e) Arewgoda, M.; Robinson, B. H.; Simpson, J. *J. Am. Chem. Soc.* **1983**, *105*, 1893. (f) Arewgoda, C. M.; Robinson, B. H.; Simpson, J. *J. Chem. Soc., Chem. Commun.* **1982**, 284.
(28) See also: Zizelman, P.; Amatore, C.; Kochi, J. K. *J. Am. Chem. Soc.* **1984**, *106*, 3771.

Scheme II

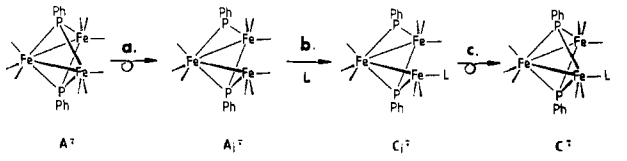

(10)

Such a mechanism derives from the transient ESR spectra of the four types of distinctive anion radicals, as described above. Thus, the spontaneous rearrangement (step a) is described by eq 4, the rapid ligand substitution (step b) is described by eq 5, and the reclosure of the phosphinidene bridge in the substitution product (step c) is the microscopic reverse of step a. The overall transformation in Scheme II corresponds to the ligand substitution of the anion radical in eq 8 as required for the electron-transfer catalysis of the parent triiron cluster, $Fe_3(PPh)_2(CO)_9$, in eq 7. The key lies in step a for the ring opening of the saturated cluster $A^{-\cdot}$ to expose a coordinatively unsaturated 17-electron iron center in $A_i^{-\cdot}$. Indeed, this formulation is in harmony with the enhanced reactivity of 17-electron metal centers in mononuclear carbonyls that are notoriously substitution-labile.[29] The mechanism in Scheme II thus focuses on the critical role of the phosphinidene cap in modulating the reactivity of the triiron cluster.

ESR studies provide evidence that fluxionality of the Fe–Fe bonds can also play a role in cluster substitution. For example, let us consider the interesting change in the ESR spectra accompanying the intramolecular ligand substitution of the pendant diphos ligand in mono-substituted $Fe_3(PPh)_2(CO)_8$(diphos) (D) by electron-transfer catalysis, i.e.

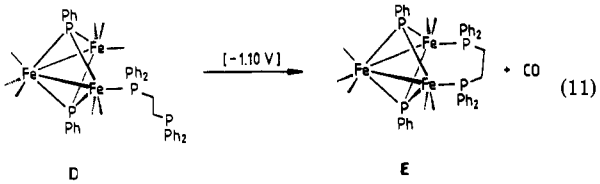

(11)

as described in Table IV, entry 3.

The ESR spectrum obtained from the reduction of D in THF is shown in Figure 4a. The ^{31}P hyperfine splittings and $\langle g \rangle$ values listed in Table III indicate that the reduced species, $D^{-\cdot}$, has maintained the cluster framework intact, i.e.

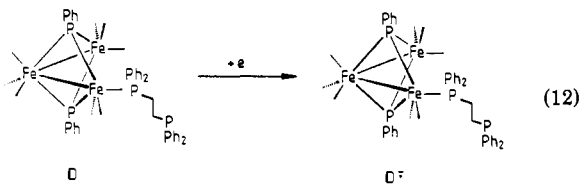

(12)

This structural assignment is supported by the similarity of $D^{-\cdot}$ to the close congener $Fe_3(PPh)_2(CO)_8PPh_3^{-\cdot}$ derived from the reduction of the triphenylphosphine derivative under the same conditions. (Compare Figure 4a with Figure 5.) The latter also establishes one terminus of the diphosphine to remain pendant upon the conversion of D to this anion radical as in eq 12. $D^{-\cdot}$ is transient and undergoes two successive structural transformations. *First*, upon standing for 30 min, it rearranges to a new anion radical, $X^{-\cdot}$. This transformation is shown by the evolution of Figure 4c, consisting simply of a 1:2:1 triplet (a_P = 13.5 G). Most notably, the ligand splitting $a_P(L)$ = 77.5 G has simply disappeared without a change in the $\langle g \rangle$ value. *Second*, anion radical $X^{-\cdot}$ is also transient, and it forms in a slower reaction (90 min) a third anion radical, $Y^{-\cdot}$, the ESR spectrum of which is shown in Figure 4d, consisting of a triplet (a_P = 12.0 G) of doublets (a_P = 81.0 G). The second transformation corresponds to an intramolecular

(29) See for leading references: (a) Walker, H. W.; Rattinger, G. B.; Belford, R. L.; Brown, T. L. *Organometallics* **1983**, *2*, 775. (b) Hershberger, J. W.; Klingler, R. J.; Kochi, J. K. *J. Am. Chem. Soc.* **1982**, *104*, 3034 and related papers.

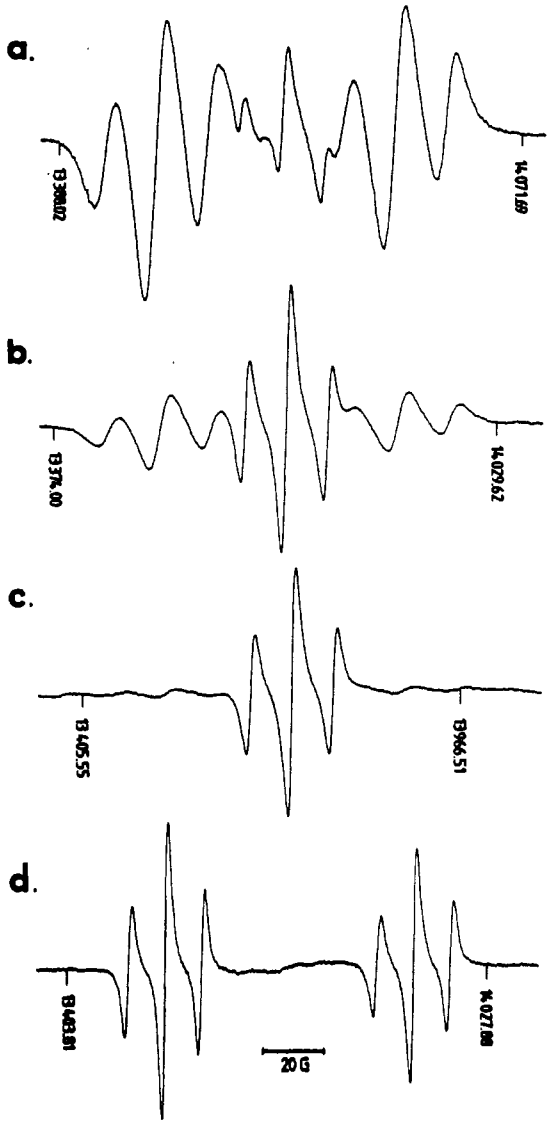

Figure 4. ESR spectra from the reduction of the mono-substituted diphos derivative $Fe_3(PPh)_2(CO)_8(PPh_2CH_2CH_2PPh_2)$ (D) with sodium amalgam in THF at 25 °C taken (a) immediately (<1 min), (b) 5 min later, (c) 30 min later, and (d) 90 min later. The principal species in (a) is $D^{-\cdot}$, in (c) is $X^{-\cdot}$, and in (d) is $Y^{-\cdot}$; (b) is a composite of (a) and (c).

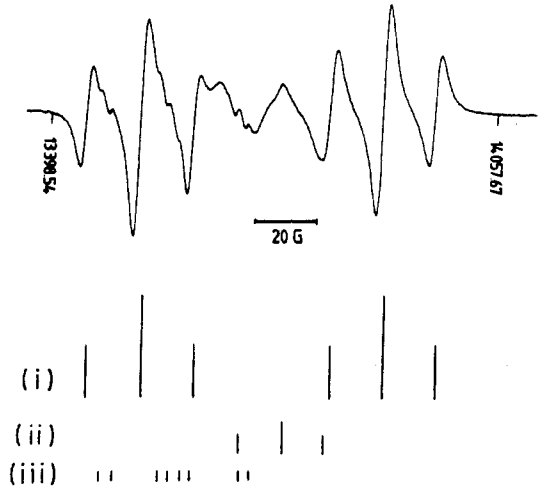

Figure 5. ESR spectrum obtained from the reduction of the mono(triphenylphosphine) derivative $Fe_3(PPh)_2(CO)_8PPh_3$ with sodium amalgam in THF at 25 °C. The stick diagrams represent the construction of (i) the principal species (basal, unopened), (ii) the minor species (apical, unopened), and (iii) the trace species (basal, opened) from the ESR parameters in Tables II and III.

ligand substitution of the pendant end of the diphos ligand, since the same ESR spectrum (Figure 4d) is obtained from the reduction of an authentic sample of bis-substitution product E. (See eq 13

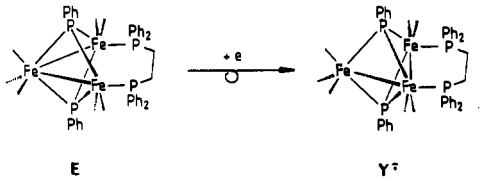

(13)

for the structure of E.) However, the ESR spectrum in Figure 4d is not consistent with a direct reduction of E to $E^{-}\cdot$. Thus, the large doublet splitting of $a_P(L) = 81$ G indicates the presence of a single phosphine ligand center in the anion radical, whereas there are two equivalent groups in E (see Experimental Section). We can resolve this ambiguity by assigning the ESR spectrum in Figure 4d to rearranged anion radical $Y^{-}\cdot$ as in eq 13. If so, first-formed anion radical $X^{-}\cdot$ (Figure 4c) could result from a similar rearrangement of $D^{-}\cdot$, i.e.

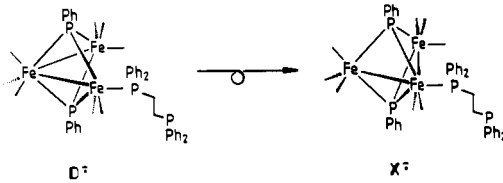

(14)

In each case, a phosphine center on a basal Fe(1) is converted into one on an apical Fe(2). Conceptually, this transformation corresponds to a valence isomerization such as

(15)

in which basal and apical Fe centers are interchanged in the anion radical. Such a transformation is analogous to the observed scrambling of osmium centers during the thermal isomerization of the trinuclear cluster, i.e.[30]

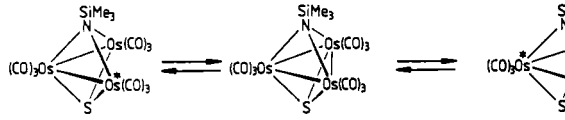

(16)

Most importantly, the structural assignments of $X^{-}\cdot$ and $Y^{-}\cdot$ from the ESR data are based on the assumption that $a_P(L)$ for a phosphine ligand attached to the apical Fe(2) center is too small to be resolved. [The analogous situation is presented in the ^{31}P NMR spectra of 1- and 2-phosphine-substituted triiron clusters, in which the spin–spin coupling constant, J_{PP}, between the phosphinidene cap and a basal phosphine is sizable (~40 Hz) but nil (<1 Hz) between the phosphinidine cap and an apical phosphine.[19]]

The sequence of interesting spectral changes in Figures 4a–c illustrates a pathway by which the intramolecular ligand substitution of diphos can occur in the course of bridging the nonbonded Fe(1) and Fe(3) centers. Critical to the understanding of this process are the identities of $X^{-}\cdot$ and $Y^{-}\cdot$, which we have speculatively presented above. The missing step in the ligand substitution of $D^{-}\cdot$ is the conversion of $X^{-}\cdot$ to $Y^{-}\cdot$ as revealed in Figure 5 by the spectral transformation c → d, i.e.

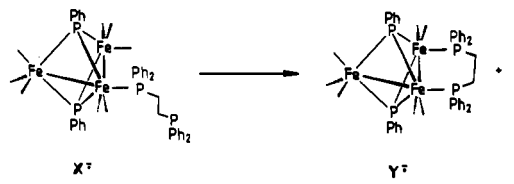

(17)

(30) Süss-Fink, G.; Thewalt, U.; Klein, H.-P. *J. Organomet. Chem.* **1982**, *224*, 59.

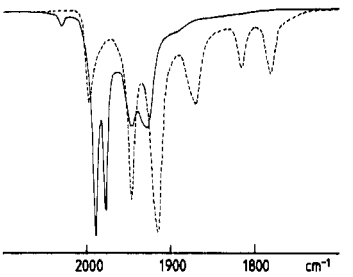

Figure 6. Comparative infrared spectra of unopened anion radical $A^{-}\cdot$ (—) and dianion A^{2-} (---) in THF at 25 °C in the ν(CO) region.

The transformation in eq 17 represents an intramolecular ligand substitution across the contiguous Fe(2)–Fe(1) centers. Such a ring closure is facilitated relative to the more direct process involving a Fe(1)–Fe(3) closure by a difference of ~0.9 Å. [Thus in A, the Fe(2)–Fe(1) bond length is 2.7 Å whereas the nonbonded Fe(1)–Fe(3) bridging distance is 3.6 Å.[8]] In other words, the sequence of steps $D^{-}\cdot \rightarrow X^{-}\cdot \rightarrow Y^{-}\cdot \rightarrow E^{-}\cdot$ is dependent on a series of "easy" valence isomerizations of the type depicted in eq 15. Despite the outward appearance of being a rather circuitous route, it may enjoy favor over the direct process (i.e., $D^{-}\cdot \rightarrow E^{-}\cdot$) by avoiding the long reach required for diphos to bridge the distant Fe(1)–Fe(3) centers in a single step. As accommodating as this rationalization is, it leaves unanswered the question as to whether the stereomutation of the triiron cluster exemplified by eq 13 and 14 occurs with other phosphine derivatives. Indeed, a close examination of the ESR spectrum in Figure 5 reveals the presence of additional lines indicative of a similar rearrangement in the triphenylphosphine derivative. Thus, the principal set of lines (i) is readily assigned to *unopened* anion radical $C^{-}\cdot$ with a basal PPh_3 ligand (Table III), and it is similar to the ESR spectrum of $D^{-}\cdot$ in Figure 4a. A minor set of lines (ii) is associated with a triplet with a splitting of similar magnitude to that of $X^{-}\cdot$ (i.e., compare spectrum ii in Figure 5 with Figure 4c). Accordingly, it is assigned to the unopened anion radical with an apical PPh_3 ligand. Finally, we associate the fine structure associated with the set of lines (iii) consisting of 3 doublets to opened anion radical $C_i^{-}\cdot$ since the magnitudes of a_P coincide with those listed in Table II. Such a mixture of anion radicals may be attributed to a facile equilibration of the triphenylphosphine ligand among (at least) three isomeric anion radicals, i.e.

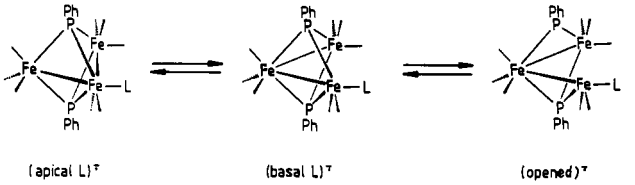

(18)

Indeed, the absence of analogous sets of lines in the spectra of anion radicals derived from triethylphosphine and trimethyl phosphite suggests that the stereomutation of basal and apical positions as in eq 18 may be induced by steric factors in monofunctional ligands. We hope that further studies will establish the validity of this interesting phenomenon.

IV. Reduction of the Triiron Cluster to the Dianion. The observation of the second reversible CV wave at $E_{1/2} = -1.30$ V in Figure 1 corresponds to the further reduction of anion radical $A^{-}\cdot$ to the diamagnetic dianion A^{2-}. The same transformation to the dark brown dianion can be performed on a preparative scale by chemical reduction in THF with either sodium naphthalene or 1% sodium amalgam. The accumulation of negative charge in the triiron cluster is reflected in Figure 6 by a red shift of ~100 cm^{-1} for the principal ν(CO) frequencies. (For example, the pair of prominent bands at 2043 and 2020 cm^{-1} in parent cluster A are shifted to 1948 and 1918 cm^{-1} in dianion A^{2-}.) An upfield shift of close to 300 ppm in the ^{31}P NMR spectrum of dianion A^{2-} relative to that of the neutral A also accords with the high electron density in the triiron cluster. Attempts to isolate the

dianion as a pure salt were unsuccessful. Moreover, coulometric measurements in THF solutions over a period of 1 h at −20 °C indicated that A^{2-} was not persistent.

The single sharp resonance at δ 31 in the ^{31}P NMR spectrum indicates that the pair of equivalent phosphinidene caps are retained in dianion A^{2-}. Such a structural situation may still persist in the teeth of the buildup of negative charge by the following consideration. According to Wade's rules,[31,32] the 5-vertex cluster such as A with 14 skeletal electrons may be regarded as a nido structure.[33] Upon 2-electron reduction, dianion A^{2-} possesses 16 skeletal electrons and should form a 5-vertex cluster regarded as an arachno structure.[33] The structural changes of the cluster core in going from the nido structure in A to the arachno structure in A^{2-} is tantamount to widening the cleft in the Fe_3P_2 framework. Although the temperature dependence of the ^{31}P NMR spectrum does not exclude a fluxional core, chemical studies indicate a preference for the steric approach of a reagent from the concave side. For example, treatment of the dianion in THF with acetic acid at −78 °C results in an instantaneous change of color to red.[34] The ^1H-decoupled ^{31}P NMR spectrum shows the presence of a pair of doublets at δ 270 and −104. The doublet at δ 270 (J_{pp} 300 Hz) is in the range typically for μ_3-phosphinidene caps (cf. Table VI). The high-field doublet at δ −104 is suggestive of a μ_2-phosphido bridge connecting two metal atoms without a metal–metal bond.[35] Furthermore this doublet shows additional splittings of 316 Hz in the ^1H-coupled ^{31}P NMR spectrum, which indicates the presence of a hydrogen atom bound to the μ_2-phosphido bridge. When the THF solution of AH^- is allowed to warm immediately to room temperature, no changes are apparent in the ^{31}P NMR spectrum. However, after the mixture is allowed to sit for 24 h at 25 °C, a new species AH'^- is observed with two sets of resonances at δ 265 (d, J_{pp} = 317 Hz) and δ −105 (t, J_{pp} = 317 Hz, J_{PH} = 317 Hz). The infrared spectrum shows no significant changes[5c] during the conversion of AH^- to AH'^-. We find that AH'^- is identical with the product previously derived from hydride addition to parent cluster A.[14] Fortunately, the overall transformation shown in eq 19 was established by an X-ray crystallographic determination of AH'^- by O'Connor.[14]

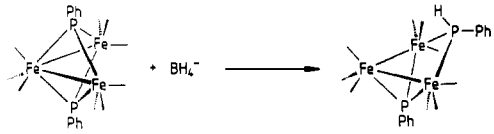

A AH'^- (19)

In order to establish the relationship between the products derived from these two diverse methods, we repeated the original procedure and carefully monitored its progress by ^{31}P NMR spectroscopy. Thus, the treatment of $Fe_3(PPh)_2(CO)_9$ with sodium borohydride in THF at room temperature leads immediately to a dark red solution. The fast reaction is accompanied in the ^1H-decoupled ^{31}P NMR spectrum by the replacement of the singlet resonance at δ 317 with a pair of doublets at δ 270 and −104, which are identical with those observed for AH^- as described above. The identity of the two was established by the comparison of the IR spectrum of the hydride product [ν(CO) 2031 (w), 1997 (s), 1962 (s), 1954 (m), 1931 (m), and 1900 (w) cm^{-1}] with that derived from the protonation of the dianion (Table I). Moreover, the ^{31}P NMR spectrum underwent the same change as that [^{31}P NMR ($CDCl_3$): δ 265 (d, J_{pp} = 317 Hz), −105 (t, J_{pp} = 317 Hz] corresponding to AH'^- from the rearrangement of the protonation product.

Scheme III

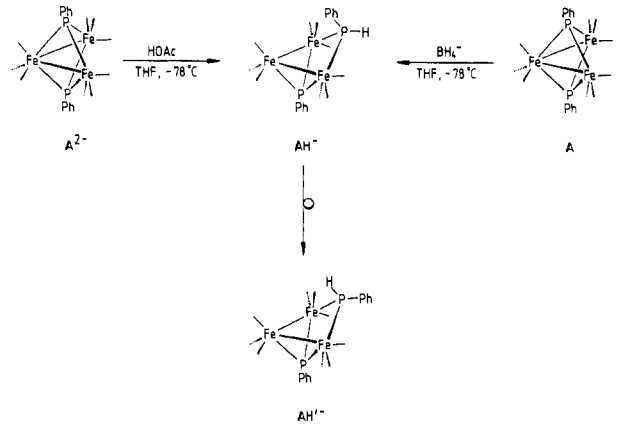

These parallel studies thus establish the same intermediate (AH^-) and the same product (AH'^-) to be derived from (a) the protonation of triiron cluster dianion A^{2-} and (b) the hydride attack on parent triiron cluster A. Such a commonality of pathways is depicted in the sequence of structural changes in Scheme III. According to Scheme III, the initially formed intermediate AH^- derives from both the protonation of A^{2-} and hydride attack on A at a phosphinidene cap from the concave side of the triiron cluster to afford the phenyl group in an endo configuration. This kinetically controlled product then slowly isomerizes to the thermodynamically formed product AH'^- in which an *exo*-phenyl group suffers diminished steric hindrance. Such a rearrangement accords with the absence of any significant change in the infrared spectrum and only a slight shift of the resonances in the ^{31}P NMR spectrum.

Finally, we wish to comment briefly on the endo–exo rearrangement of the phosphido bridge during the conversion of AH^- to AH'^- in Scheme III. Such a facile rearrangement could occur via a deprotonation followed by a pyramidal inversion at phosphorus and reprotonation. In order to test this possibility, we treated triiron cluster A with 1 equiv of methyllithium in THF at −78 °C. Upon warming of the solution to room temperature, the ^{31}P NMR spectrum showed the appearance of a pair of doublets at δ 271 and −102 (J_{pp} = 324 Hz). No other phosphorus-containing species could be detected. The infrared spectrum of the red-brown solution in the carbonyl region was the same (Table I) as that of AH'^- but consistently red-shifted by 3–4 cm^{-1}. Within 24 h the ^{31}P NMR spectrum was converted to a new set of slightly displaced resonances at δ 257 and −104 (J_{pp} = 344 Hz), reminiscent of the change from AH^- to AH'^-. We conclude from these experiments that the endo → exo rearrangement probably occurs by a unimolecular pathway related to those observed in organic and organometallic systems.[36,37]

Summary and Conclusion

The reduction of the triiron cluster $Fe_3(\mu_3\text{-}PPh)_2(CO)_9$ (A) occurs in two well-defined 1-electron steps to generate the anion radical $A^{-\cdot}$, and the dianion, A^{2-}, without substantial changes in the cluster framework. The anion radical is a labile species undergoing a series of interesting transformations, especially during electron-transfer catalysis. The study of $A^{-\cdot}$ is made possible by transient ESR spectroscopy since the ^{31}P hyperfine splittings of the phosphinidene caps are well resolved in the intermediates. The slippage of the phosphinidene cap from μ_3 to μ_2 coordination plays an important role in cluster activation, as depicted in Scheme II. Stereomutation of the Fe_3 core (eq 15) is delineated during the intramolecular ligand substitution of the diphos derivative by ETC.

Hydridic attack on triiron cluster A occurs only at the phosphinidene since no formyl- or hydridoiron species could be detected even at −70 °C with either sodium borohydride or sodium triethylborohydride. Similarly, the protonation of dianion A^{2-} also

(31) Wade, K. *Adv. Inorg. Chem. Radiochem.* **1976**, 18.
(32) See also: Wade, K. In *Transition Metal Clusters*; Johnson, B. F. G., Ed.; Wiley: New York, 1980; Chapter 3.
(33) According to these rules, the nido structure is derived from a closo 6-vertex structure by removal of a vertex. Similarly, the arachno structure is derived from the closo 7-vertex structure by removal of a pair of adjacent basal vertices.
(34) Cf. also ref 15 and: Knoll, K.; Hüttner, G.; Wasiucionek, M.; Zsolnai, L. *Angew. Chem., Int. Ed. Engl.* **1984**, *23*, 739.
(35) Garrou, P. E. *Chem. Rev.* **1981**, *81*, 229.
(36) Berson, J. A. *Acc. Chem. Res.* **1968**, *1*, 152.
(37) Cotton, F. A.; Wilkinson, G. *Advanced Inorganic Chemistry*, 4th ed.; Wiley: New York, 1980; p 1217 ff.

Table VI. ^{31}P NMR Spectra of the Triiron Clusters[a]

triiron cluster	isomer[b]	$\delta(^{31}P\{^1H\})$[c] μ_3-PPh	ligand 1	ligand 2
$Fe_3(PPh)_2(CO)_9$ (A)		317.0 (s)		
$Fe_3(PPh)_2(CO)_8PEt_3$[d] (B)	I	283.7 (d, 39)	60.9 (t, 39)	
	II	312.0 (s)	49.2 (s)	
$Fe_3(PPh)_2(CO)_7(PEt_3)_2$[d]	III	282.0 (d, 34)	56.3 (t, 34)	48.4 (s)
$Fe_3(PPh)_2(CO)_8P(OMe)_3$[d]	I	299.1 (d, 46)	182.0 (t, 46)	
	II	317.0 (s)	183.4 (s)	
$Fe_3(PPh)_2(CO)_7[P(OMe)_3]_2$[d]	III	299.0 (d, 39)	184.1 (t, 39)	186.8 (s)
	IV	264.7 (t, 39)	185.4 (t, 39)	
$Fe_3(PPh)_2(CO)_8PPh_3$	I	291.2 (d, 29)	72.9 (t, 29)	
$Fe_3(PPh)_2(CO)_8(Ph_2PCH_2)_2$ (D)	I	287.5 (d, 34)	63.0 (dt, 44, 34)	−13.0 (d, 44)
$Fe_3(PPh)_2(CO)_7(Ph_2PCH_2)_2$ (E)	IV	283.4 (t, 34)	66.7 (t, 34)	

[a] In $CDCl_3$. [b] P ligand: (I) on Fe(1); (II) on Fe(2); (III) on [Fe(1), Fe(2)]; (IV) on [Fe(1), Fe(3)]. [c] J_{pp} (Hz) in parentheses. [d] From ref 19.

occurs directly only at the phosphinidene bridge. Such an identity demonstrates that the site of cluster reactivity can be reversed upon a 2-electron change, which converts the phosphinidene from an electrophilic center in A to a nucleophilic center in A^{2-}. Essentially the same point derives from the reactivity of anion radical $A^{-\cdot}$ which must cleave a Fe–P bond prior to reaction at an iron center. The behavior of all three species, A, $A^{-\cdot}$, and A^{2-}, thus underscores the critical role of the bridging phosphinidene cap in cluster reactivity.

Experimental Section

Materials. $Fe_3(PPh)_2(CO)_9$ was prepared from iron pentacarbonyl and phenyldichlorophosphine (Strem Chemical) by the procedure described by Muetterties et al;[7] mp 132–134 °C. $^{31}P\{^1H\}$ NMR ($CDCl_3$): δ 317 (s). IR (hexane), ν(CO): 2044 (s), 2023 (s), 2008 (s), 1996 (m), 1986 (w) cm^{-1}. Trimethyl phosphite (Victor Chemical), triphenylphosphine (Matheson), triethylphosphine (Pressure Chemical), tri-*p*-tolylphosphine and trianisylphosphine (M and T Chemical), and methyldiphenylphosphine (Organometallics) were further purified by either distillation or sublimation and stored under argon. Ethyldiphenylphosphine, diethylphenylphosphine, dimethylphenylphosphine, *n*-butoxydiphenylphosphine, and bis(*n*-butoxy)phenylphosphine were prepared from the treatment of chlorodiphenylphosphine and dichlorophenylphosphine with either the appropriate Grignard reagent or sodium alkoxide. The other phosphines and phosphites were from previous studies.[28] Tetra-*n*-butylammonium perchlorate (G. F. Smith Chemical) was recrystallized from a mixture of hexane and ethyl acetate and dried in vacuo prior to use. Silica gel (60–200) mesh from J. T. Baker was used for column chromatography.

All manipulations were carried out under argon with the aid of standard Schlenk line techniques. Solvents were purified by standard procedures.[38] Melting points are not corrected. Elemental analyses were performed by Atlantic Microlab, Inc., Atlanta, GA.

Synthesis of $Fe_3(PPh)_2(CO)_8PPh_3$. To an argon-filled electrolysis cell was added 200 mg (0.314 mmol) of $Fe_3(PPh)_2(CO)_9$ (A) followed by 25 mL of THF containing 0.3 M TBAP and 157 mg (0.600 mmol) of triphenylphosphine. The electrocatalytic reaction was initiated by the passage of ~2.0 mA of cathodic current in a constant-current mode through the stirred solution. The initial potential of −0.79 V shifted to −0.88 V during the passage of 20% of the theoretical charge required for the amount of A charged. The extent of the ligand substitution was monitored by cyclic voltammetry. After 2 h at 25 °C, it was complete and the solution ws reoxidized by passage of ~2.0 mA of anodic current in a constant-current mode until the potential had shifted to −0.2 V. The electrolysate was evaporated to dryness (in vacuo), and the residue was extracted with a 1:1 mixture of benzene and hexane. After filtration through 3 cm of silica gel, the filtrate was concentrated. Chromatography through a 3 × 10 cm column of silica gel with a 2:1 mixture of hexane and benzene yielded a dark brown solid. Recrystallization from a 5:1 mixture of hexane and toluene yielded 123 mg (45%) of dark violet crystals of $Fe_3(PPh)_2(CO)_8PPh_3$, mp 194 °C. The IR and NMR spectral data agreed with those reported previously.[7]

Synthesis of $Fe_3(PPh)_2(CO)_8(Ph_2PCH_2)_2$ (D). The electrosynthesis followed a procedure similar to that described above in THF containing 0.3 M TBAP starting with 200 mg (0.314 mmol) of A and 250 mg (0.630 mmol) of diphos. The electroreduction was carried out at −0.8 V by passage of 2.0 mA until a total charge of 10% was passed. Workup in the usual manner yielded a product that was purified on a 3 × 10 cm column of silica gel with a 2:1 mixture of hexane and benzene. Crystallization from hexane yielded 122 mg (38%) of red microcrystalline $Fe_3(PPh)_2(CO)_8(Ph_2PCH_2)_2$, mp 133–135 °C. ^1H NMR ($CDCl_3$): δ 7.8–6.7 (m, C_6H_5), 2.8–2.4 (m, CH_2), 1.8–1.4 (m, CH_2). $^{31}P\{^1H\}$ NMR ($CDCl_3$): δ 287.65 (d,(μ_3-PPh), $^2J_{PP}$ = 34.2 Hz), 63.0 (dt, (Fe–PPh_2CH_2), $^2J_{PP}$ = 34.2 Hz, $^3J_{PP}$ = 43.9 Hz), −13.0 (d (Ph_2PCH_2–), $^3J_{PP}$ = 43.9 Hz). IR (ν(CO), toluene): 2054 (s), 2011 (s), 1990 (s), 1972 (w), 1948 (m) cm^{-1}. Anal. Calcd for $C_{46}H_{34}Fe_3O_8P_4$ (M_r = 1006.2): C, 54.91; H, 3.41. Found: C, 55.04; H, 3.46.

Synthesis of $Fe_3(PPh)_2(CO)_7(Ph_2PCH_2)_2$ (E). The synthesis followed a procedure similar to that described above in THF containing 0.3 M TBAP starting with 200 mg (0.314 mmol) of A and 250 mg (0.630 mmol) of diphos. Electrocatalysis was initiated at −0.80 V until 10% charge was passed and then at −1.10 V until 60% charge was passed. An anodic current was then passed through the electrolysate until the potential of −0.2 V was attained. Workup as usual afforded a product that was purified by chromatography on a 3 × 10 cm column of silica gel with a 1:1 mixture of hexane and toluene. Qualitatively, the chromatographic behavior of E is similar to that of D. Recrystallization from a mixture of hexane and methylene chloride yielded 54 mg (18%) of red microcrystalline $Fe_3(PPh)_2(CO)_7(PPh_2PCH_2)_2$, mp > 240 °C. ^1H NMR ($CDCl_3$): δ 7.8–7.2 (m, C_6H_5), 2.3 (m, CH_2). $^{31}P\{^1H\}$ NMR ($CDCl_3$): δ 283.4 (t (μ_3-PPh), $^2J_{PP}$ = 34.2 Hz), 66.7 (t (Ph_2PCH_2–), $^2J_{PP}$ = 34.2 Hz). IR (ν(CO), toluene): 2029 (s), 1991 (s), 1974 (m), 1968 (m), 1947 (w), 1938 (m) cm^{-1}. Anal. Calcd for $C_{45}H_{34}Fe_3O_7P_4$ (M_r = 978.2): C, 55.25; H, 3.50. Found: C, 56.55; H, 3.79.

Instrumentation. The ^1H (89.55-MHz) and ^{31}P (36.23-MHz) NMR spectra were recorded on a JEOL FX-90Q spectrometer. Infrared spectra were obtained on a Nicolet DX-10 FT spectrometer. The X-band ESR spectra were recorded on a Varian Century-line E112 spectrometer equipped with a NMR gaussmeter for field frequency calibration. Cyclic voltammetry was performed at a platinum electrode with an IR-compensated potentiostat driven by a Princeton Applied Research Model 175 universal programmer. The high-impedance voltage-follower amplifier was mounted external to the potentiostat to minimize the length of the connection to the reference electrode for low-noise pickup. Cyclic voltammograms were recorded on a Houston Series 2000 X-Y recorder. The $E_{1/2}$ and E_p values were determined by cyclic voltammetry and referred to SCE. The reference electrode was in contact with the solution by a cracked-glass tip. The bulk electrolysis cell was of air-tight design with high-vacuum Teflon valves (Kontes) and Viton O-ring seals to allow an inert atmosphere to be maintained without contamination by grease.

Structural Assignment of Triiron Clusters from Their ^{31}P NMR Spectra. For the triiron clusters substituted with a phosphine ligand on the basal Fe(1) center, the proton-decoupled ^{31}P NMR spectrum consists of a doublet at δ ~280–290 due to splitting ($J \simeq$ 30–40 Hz) by the phosphorus ligand showing a triplet splitting ($J \sim$ 30–40 Hz) with chemical shifts that are strongly dependent on the ligand structure.[19] (Furthermore, the ^{31}P NMR spectra of phosphine derivatives substituted on an apical Fe(2) center consist of a singlet at δ ~310 for the phosphinidene cap and a singlet whose chemical shift is highly dependent on the ligand substitution (e.g., δ 183 and 49 for the $P(OMe)_3$ and PEt_3 derivatives, respectively).)[19] The ^{31}P spectral data for the triphenylphosphine derivative and mono-coordinated diphos derivative D in Table VI are consistent with these trends. In addition, for D another doublet occurs at δ −13.0 for the pendant $-CH_2PPh_2$ group. The formation of such a mono-coordinated diphos during ETC ligand substitution of $Fe_3(CO)_9(PPh)_2$ is in contrast to that observed with the tricobalt cluster $Co_3(\mu_3\text{-}CPh)(CO)_9$ and diphos which leads to a product with two cluster

(38) Perrin, D. D.; Armarego, W. L.; Perrin, D. R. *Purification of Laboratory Chemicals*; Pergamon: New York, 1980.

units bridged by a difunctional diphos ligand.[39]

The ^{31}P NMR spectrum of bis-substituted E consists of a well-resolved 1:2:1 triplet at δ 283.4 for the two phosphinidene caps and another well-resolved 1:2:1 triplet at δ 66.7 for the two coordinated phosphine ligands, with both triplets of equal intensity. The mass spectrometric determination of the molecular weight of *m/e* 986 precludes a dimeric structure for E. The ligand can be bis-coordinated to the triiron cluster in three possible ways, i.e., diphos chelating the Fe(1) center, bridging the Fe(1) and Fe(2) centers, or bridging the Fe(1) and Fe(3) centers, which we designate as isomers a, b, and c, respectively. Isomer b can be rejected on the basis of the observed triplet splitting at δ 66.7, which indicates the presence of two equivalent phosphine ligand centers on E. [Note that phosphine ligands and Fe(1) and Fe(2) on triiron clusters cannot be accidentally degenerate (see Table V). Isomer a consists of diphos in a 5-membered ring, whereas isomer c has it in a quasi-6-membered ring. Garrou[35,40] has shown that the phosphorus coordination to a metal in a 5-membered chelate ring is highly shielded. Thus, the ring effect parameter, $\Delta_r = \delta(L_{coord}) - \delta(L_{free})$, is large and positive for 5-membered rings, highly negative for 4-membered rings, and close to zero or weakly negative for 6-membered rings. Evaluated in this way, triiron cluster E with $\Delta_r = +3.7$ is the 6-membered isomer c. Although we were able to grow a single crystal of E as a fine dark red needle, it was unfortunately not suitable for X-ray crystallography. Barring our extensive efforts to grow another crystal modification, we rely on the ^{31}P NMR spectral analysis for the structural assignment of E.

ESR Spectroscopy. Solutions of the closed anion radicals (Table III) were prepared by reduction of the triiron cluster with 1% sodium amalgam in tetrahydrofuran or acetonitrile. The reduction of $Fe_3(PPh)_2(CO)_9$ (A) by cobaltocene in acetonitrile also afforded the closed anion radical $A^{-}\cdot$. The ESR spectrum of $A^{-}\cdot$ shown in Figure 3a is essentially the same as that obtained in THF by the sodium amalgam reduction (vide supra). Upon standing, $A^{-}\cdot$ rearranges to open species $A_i^{-}\cdot$ showing the ESR spectrum in Figure 2a. The substituted derivatives $C_i^{-}\cdot$ presented in Table I were generated in situ by the addition of the appropriate phosphine. The same ESR spectra were obtained by the sodium amalgam reduction of the triiron cluster $Fe_3(PPh)_2(CO)_8L$ in acetonitrile and by allowing the solution to stand. The solutions of the anion radicals were transferred with the aid of a hypodermic syringe into ESR tubes that were then sealed in vacuo. For the description of the ESR technique, see ref 41.

Acknowledgment. We thank the National Science Foundation and the Robert A. Welch Foundation for financial support. H. H. Ohst is a recipient of a NATO grant administered under the auspices of the German Academic Exchange Service.

Registry No. A, 38903-71-8; A^{-}, 101198-33-8; A^{2-}, 102000-25-9; A_i^{-}, 101011-28-3; AH^{-}, 102046-68-4; AH'^{-}, 102000-51-1; AMe^{-}, 102046-69-5; B (isomer I), 101011-19-2; B (isomer II), 102000-28-2; C (L = $P(OMe)_3$, isomer I), 39040-36-3; C (L = $P(OMe)_3$, isomer II), 102000-29-3; C (L = PPh_3), 102130-35-8; $C^{-}\cdot$ (L = PEt_3), 101011-27-2; $C^{-}\cdot$ (L = $P(OMe)_3$), 101011-23-8; $C^{-}\cdot$ (L = PPh_3), 101011-22-7; $C_i^{-}\cdot$ (L = PPh_3), 101011-24-9; $C_i^{-}\cdot$ (L = $P(p\text{-}ClC_6H_4)_3$), 102000-35-1; $C_i^{-}\cdot$ (L = $P(p\text{-}MeC_6H_4)_3$), 102046-67-3; $C_i^{-}\cdot$ (L = $P(p\text{-}MeOC_6H_4)_3$), 102000-36-2; $C_i^{-}\cdot$ (L = PPh_2Et), 102000-38-4; $C_i^{-}\cdot$ (L = PPh_2Me), 102000-39-5; $C_i^{-}\cdot$ (L = $PPhEt_2$), 102000-40-8; $C_i^{-}\cdot$ (L = $PPhMe_2$), 102000-41-9; $C_i^{-}\cdot$ (L = PEt_3), 101011-25-0; $C_i^{-}\cdot$ (L = $P(i\text{-}Pr)_3$), 102000-42-0; $C_i^{-}\cdot$ (L = PBu_3), 102000-43-1; $C_i^{-}\cdot$ (L = $P(c\text{-}C_6H_{11})_3$), 102000-44-2; $C_i^{-}\cdot$ (L = $PPh_2(OBu)$), 102000-45-3; $C_i^{-}\cdot$ (L = $PPh(OBu)_2$), 102000-46-4; $C_i^{-}\cdot$ (L = $P(OPh)_3$), 102000-47-5; $C_i^{-}\cdot$ (L = $P(OMe)_3$), 102000-48-6; $C_i^{-}\cdot$ (L = $P(O\text{-}i\text{-}Pr)_3$), 102000-49-7; $C_i^{-}\cdot$ (L = $AsPh_3$), 102000-50-0; D (isomer I), 102000-26-0; D^{-} (isomer I), 102000-32-8; $D^{-}\cdot$ (isomer II), 102000-33-9; $D_i^{-}\cdot$ (isomer I), 102000-37-3; E (isomer IV), 102000-27-1; $E^{-}\cdot$ (isomer IV), 102000-34-0; $Fe_3(PPh)_2(CO)_7[P(OMe)_3]_2$ (isomer III), 102000-30-6; $Fe_3(PPh)_2(CO)_7[P(OMe)_3]_2$ (isomer IV), 102000-31-7; $Fe_3(PPh)_2(CO)_7(PEt_3)_2$ (isomer III), 102046-70-8; CH_3CO_2H, 64-19-7; Fe, 7439-89-6; P, 7723-14-0.

(39) Cunninghame, R. G.; Downard, A. J.; Hanton, L. R.; Jensen, S. D.; Robinson, B. H.; Simpson, J. *Organometallics* **1984**, *3*, 180.
(40) Garrou, P. E. *Inorg. Chem.* **1975**, *14*, 1435.
(41) Lau, W.; Huffman, J. C.; Kochi, J. K. *Organometallics* **1982**, *1*, 155.

Contribution from the Department of Chemistry, The University of Houston, University Park, Houston, Texas 77004

Electrochemistry of $Mn_2(CO)_{10}$, $[Mn(CO)_5]^+$, $[Mn(CO)_5]^-$, and $Mn(CO)_5$

D. A. Lacombe, J. E. Anderson, and K. M. Kadish*

Received November 4, 1985

A self-consistent electrochemical mechanism for the reduction and oxidation of the $Mn_2(CO)_{10}$ metal–metal bonded dimer, and the associated monomeric $[Mn(CO)_5]^+$ and $[Mn(CO)_5]^-$ ions, was determined by the use of various electrochemical methods. The dimer is both reduced and oxidized by an overall two electrons with the initial step being the formation of the monomeric 17-electron $Mn(CO)_5$ radical. This radical was shown to be a key intermediate species in all of the electrochemical oxidations and reductions. It was also shown that the $[Mn(CO)_5]^-$ and $[Mn(CO)_5]^+$ ions could be directly interconverted via an overall two-electron-transfer sequence that passed through the $Mn(CO)_5$ species. This type of reactivity has not previously been reported.

Introduction

The electrochemistry of organometallic metal–metal bonded complexes has been the object of many studies over the last 20 years.[1-10] Numerous dimers of the form M_2L_2 have been examined where M is a metal or metalate ion and L is the set of ligands of the form $(CO)_x(\eta^5\text{-}C_5H_5)_y$. Perhaps the most studied complex of this type is $Mn_2(CO)_{10}$. This complex may be oxidized in nonaqueous media by two electrons[4] to yield $[Mn(CO)_5]^+$, or the dimer may be reduced by two electrons[1-4,11-13] to yield $[Mn(CO)_5]^-$. The 17-electron $Mn(CO)_5$ radical may also be photochemically generated from $Mn_2(CO)_{10}$, and the characterization and reactivity of this radical has been the object of numerous studies.[14-28]

(1) Dessy, R. E.; Stary, F. E.; King, R. B.; Waldrop, W. *J. Am. Chem. Soc.* **1966**, *88*, 471.
(2) Dessy, R. E.; Weissman, P. M.; Pohl, R. L. *J. Am. Chem. Soc.* **1966**, *88*, 5117.
(3) Lemoine, P.; Giraudeau, A.; Gross, M. *Electrochim. Acta* **1976**, *21*, 1.
(4) Pickett, C. J.; Pletcher, D. *J. Chem. Soc., Dalton Trans.* **1975**, 879.
(5) Denisovitch, L. I.; Gubin, S. P.; Chapovskii, Y. A.; Ustynok, N. A. *Bull. Acad. Sci. USSR, Div. Chem. Sci. (Engl. Transl.)* **1971**, *20*, 1851.
(6) Madach, T.; Vahrenkamp, H. *Z. Naturforsch., B: Anorg. Chem., Org. Chem.* **1979**, *34B*, 573.
(7) Ferguson, J. A.; Meyer, T. J. *Inorg. Chem.* **1971**, *10*, 1025.
(8) Miholova, D.; Vlcek, A. A. *Inorg. Chim. Acta* **1980**, *41*, 119.
(9) de Montauzon, D.; Poilblanc, R.; Lemoine, P.; Gross, M. *Electrochim. Acta* **1978**, *23*, 1247.
(10) Connelly, N. G.; Geiger, W. E. *Adv. Organomet. Chem.* **1984**, *23*, 1.
(11) Colton, R.; Dalziel, J.; Griffith, W. P.; Wilkinson, G. *J. Chem. Soc.* **1960**, 71.
(12) Denisovich, L. I.; Ioganson, A. A.; Gubin, S. P.; Kolobova, N. E.; Anisimov, K. N. *Bull. Acad. Sci. USSR, Div. Chem. Sci. (Engl. Transl.)* **1969**, *18*, 218.
(13) Lemoine, P.; Gross, M. *J. Organomet. Chem.* **1977**, *133*, 193.
(14) Walker, H. W.; Herrick, R. S.; Olsen, R. J.; Brown, T. L. *Inorg. Chem.* **1984**, *23*, 3748.
(15) Wagman, R. W.; Olsen, R. J.; Gard, D. R.; Faulkner, L. R.; Brown, T. L. *J. Am. Chem. Soc.* **1981**, *103*, 6089.
(16) Hughey, J. L.; Anderson, C. P.; Meyer, T. J. *J. Organomet. Chem.* **1977**, *125*, C49.

0020-1669/86/1325-2074$01.50/0